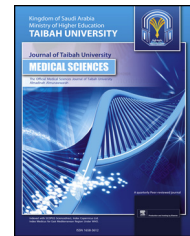




# Taibah University

## Journal of Taibah University Medical Sciences

www.sciencedirect.com



Original Article

## Protective effect of lycopene against celecoxib induced fat deposition and glycogen reduction in liver cells

Maria Khan, M.Phil.<sup>a</sup>, Somia Gul, PhD<sup>b,\*</sup>, Iqra Rehman, M.Phil.<sup>b</sup>,  
Qurratul-ain Leghari, PhD<sup>c</sup>, Rabia Badar, PhD<sup>d</sup> and Zille-Huma, FCPS<sup>e</sup>

<sup>a</sup> Department of Anatomy, Dr. Ishrat-ul-Ebad Khan Institute of Oral Health Sciences, Dow University of Health Sciences, Karachi, Pakistan

<sup>b</sup> Department of Pharmaceutical Chemistry, Faculty of Pharmacy, Jinnah University for Women, Karachi, Pakistan

<sup>c</sup> Department of Pharmaceutical Chemistry, Faculty of Pharmacy, Hamdard University, Karachi, Pakistan

<sup>d</sup> Department of Botany, Faculty of Science, Jinnah University for Women, Karachi, Pakistan

<sup>e</sup> Department of Medicine, Dow University of Health Sciences, Karachi, Pakistan

Received 7 May 2024; revised 21 June 2024; accepted 26 July 2024; Available online 8 August 2024



### المخلص

**أهداف البحث:** يتطور الإجهاد التأكسدي بسبب اضطراب في توازن مضادات الأكسدة الداعمة للأول ويمكن وصفه بأنه اضطراب في إشارات الأكسدة والاختزال والتحكم فيها. يعد السيليكوكسيب، وهو مثبط انتقائي لـ"كوكس-2"، دواء فعالاً لتسكين الألم والالتهاب. ومع ذلك، ثبت أن السيليكوكسيب يسبب إصابة مؤكسدة للأنسجة الكبدية عن طريق بيروكسيد الدهون المعزز الذي يؤدي إلى الإنتاج المفرط لأنواع الأكسجين التفاعلية. ولذلك فإن استخدامه المتكرر أو على المدى الطويل قد يؤدي إلى آثار جانبية كبدية وكلوية وغيرها من الآثار الجانبية الملحوظة. الليكوبين (لايكو) هو أحد مضادات الأكسدة القوية التي تتواجد بشكل طبيعي في الفواكه والخضروات المصبوغة. وهو مزيج نشط للأكسجين المفرد والجذور الحرة الأخرى وبالتالي حماية الخلايا من هدم غشاء البلازما الذي تسببه الجذور الحرة.

**طريقة البحث:** افترضت الدراسة أن اللايكو قد يحمي خلايا كبد الفئران من الإجهاد التأكسدي الناتج عن السيليكوكسيب، مما يقلل من تسلسل الدهون واستنفاد الجليكوجين. تم تقسيم الفئران بشكل عشوائي إلى ثلاث مجموعات (10 فئران / مجموعة): المجموعة الضابطة أ (المحلول الملحي فقط)، المجموعة ب السيليكوكسيب (50 مجم / كجم، عن طريق الفم)، المجموعة ج السيليكوكسيب+اللايكو (50 مجم / كجم، عن طريق الفم) لمدة 30 يوماً. بعد ذلك، تم فحص أنسجة الكبد لمعرفة متوسط وزن الكبد والتغيرات النسيجية في محتوى الدهون والجليكوجين.

**النتائج:** خفف اللايكو من تلف خلايا الكبد في الفئران المعالجة بـ السيليكوكسيب، مما قلل من تراكم الدهون وفقدان الجليكوجين، على الأرجح من خلال خصائصه المضادة للأكسدة. يمكن أن يؤدي تناول اللايكو و السيليكوكسيب المصاحب إلى منع الآثار الجانبية السامة للكبد فيما يتعلق بالإصابة التأكسدية التي يتبعها مرض الكبد الدهني غير الكحولي، وهو أحد مكونات متلازمة التمثيل الغذائي الرئيسية. علاوة على ذلك، كشف اتجاه ربط اللايكوبين في موقع الربط لإنزيم "كوكس-2" أن المركب المرسي أظهر قوة ربط كبيرة.

**الاستنتاجات:** في الختام، تكشف دراستنا عن سلوك حماية اللايكوبين ضد تلف الكبد الناتج عن السيليكوكسيب عن طريق تقليل استنزاف الدهون والجليكوجين.

**الكلمات المفتاحية:** السيليكوكسيب؛ دراسات الالتحام؛ التتبع الدهني؛ استنزاف الجليكوجين؛ اللايكوبين؛ منتج طبيعي

### Abstract

**Objective:** Oxidative stress develops because of a shift in the prooxidant–antioxidant balance toward the former, because of disturbances in redox signaling and control. Celecoxib (Cb), a selective COX-2 inhibitor, is a drug that effectively decreases pain and inflammation. However, Cb causes oxidative injury to hepatic tissues via enhanced lipid peroxidation, thus resulting in excessive production of reactive oxygen species. Consequently, frequent or long-term Cb use may lead to hepatic, renal, and other noticeable adverse effects. Lycopene (lyco), a potent antioxidant naturally occurring in pigmented fruits and vegetables, actively eradicates singlet oxygen and other free radicals, thereby protecting cells against destruction of the plasma membrane by free radicals.

\* Corresponding address: Department of Pharmaceutical Chemistry, Faculty of Pharmacy, Jinnah University for Women, Karachi, 74600, Pakistan.

E-mail: drsomi1983@yahoo.com (S. Gul)

Peer review under responsibility of Taibah University.



Production and hosting by Elsevier

**Methods:** We hypothesized that lyco might protect rat liver cells against Cb-induced oxidative stress, thus reducing fatty infiltration and glycogen depletion. Rats were randomized into three groups (with ten rats each) receiving control (group A, saline only), Cb (group B, 50 mg/kg, orally), or Cb + lyco (group C, 50 mg/kg, orally) for 30 days. Subsequently, liver tissues were examined, and the average liver weight and histological changes in fat and glycogen content were determined.

**Results:** Lyco mitigated hepatocyte damage in Cb-treated rats, reducing fat accumulation and glycogen loss, probably through its antioxidant properties. Concomitant lyco and Cb intake prevented hepatotoxic adverse effects due to oxidative injury, as well as non-alcoholic fatty liver disease (NAFLD), a key component of metabolic syndrome. Moreover, the binding orientation of lyco in the binding site of COX-2 enzyme revealed that the docked complex had noteworthy binding strength.

**Conclusion:** In conclusion, our study revealed lyco's protective effects against Cb-induced hepatic damage by reducing fat and glycogen depletion.

**Keywords:** Celecoxib; Docking studies; Fatty degeneration; Glycogen depletion; Lycopene; Natural product

© 2024 The Authors. Published by Elsevier B.V. This is an open access article under the CC BY-NC-ND license (<http://creativecommons.org/licenses/by-nc-nd/4.0/>).

## Introduction

In vitro models or systems are critical in cellular medicine, because they provide an accurate understanding of the behavior of a cell or microorganism. However, because the cells and microorganisms are outside their natural environment, these models might not fully or precisely demonstrate the effects of chemicals, such as drugs or environmental pollutants, on the whole organism.<sup>1</sup> Despite the altering approach of experimental research toward in vitro systems, animal models still remain the “gold standard”,<sup>2</sup> because, although they might not accurately indicate drugs' toxicological effects because of inter-species differences, they provide a preliminary foundation for more advanced study or evaluation of parameters, e.g., through in vitro or in silico models, or organ-on-a-chip techniques.<sup>3</sup>

Non-steroidal anti-inflammatory drugs (NSAIDs) are drugs routinely prescribed by physicians or used as self-medication for the management of pain and inflammation, despite their well-known and pronounced adverse effects.<sup>4</sup> NSAIDs are non-selective COX enzyme inhibitors that elicit several adverse effects.<sup>5</sup> Selective COX-2 inhibitors are preferred over NSAIDs for long-term treatment of pain and inflammation due to diseases, because they exhibit lesser adverse effects and avoid the most common gastrointestinal side effects of NSAIDs, such as peptic ulcers and gastrointestinal mucosal damage.<sup>6</sup>

Celecoxib (Cb), as illustrated in Figure 1(a), is a non-steroidal anti-inflammatory drug that selectively inhibits COX-2, and is frequently used as an analgesic, anti-inflammatory, and antipyretic agent.<sup>7</sup> Generally, Cb is used to manage acute and chronic pain and inflammatory conditions such as osteoarthritis, rheumatoid arthritis, and dental pain.<sup>8</sup> Cyclooxygenase (COX) plays a key role in the synthesis of prostaglandin inflammatory mediators, which stimulate the inflammatory pathway that ultimately causes inflammation and pain. The COX enzyme has two isoforms: cyclooxygenase-1 (COX-1) and cyclooxygenase-2 (COX-2).<sup>9</sup> Inflammatory and pain responses are due to the action of COX-2 enzyme, whose inhibition is responsible for the therapeutic effects of NSAIDs, whereas COX-1 inhibition gives rise to the gastrointestinal, hepatic, and renal adverse effects of non-selective NSAIDs.<sup>10</sup> Because COX-2 inhibitors elicit lesser adverse effects than NSAIDs, physicians prefer to prescribe selective COX-2 inhibitors for long-term treatment of pain and inflammation in diseases.<sup>11</sup> However, Cb has been demonstrated to cause oxidative injury to tissue by increasing lipid peroxidation and inhibiting oxidative phosphorylation, thus resulting in the formation of reactive oxygen species (ROS).<sup>12</sup> Oxidative stress indicates an imbalance between ROS production and the capacity of the antioxidant system, and is considered the main contributor to liver injury in conditions such as NAFLD. ROS, such as superoxide anion radicals ( $O_2^{\bullet-}$ ) and hydrogen peroxide ( $H_2O_2$ ), are continuously formed intracellularly as byproducts of active metabolism in liver cells. Excess lipids in various liver cells promote excessive formation of oxidants via several ROS-producing mechanisms. Thus, high levels of ROS cause oxidative transformation of cellular biomolecules including lipids and proteins, and consequently lead to aggregation of injured macromolecules and liver injury. The mechanisms through which ROS facilitate fatty liver development may involve both undifferentiating oxidative biomolecular injury and impaired redox signaling; however, the exact molecular pathways are not yet clear.<sup>13</sup> Long-term therapy with Cb is also associated with adverse effects such as hepatotoxicity, nephrotoxicity, allergic reactions, and hypertension, depending on treatment dosage and duration.<sup>14</sup>

Antioxidants are essential in protecting cells and their organelles against the oxidative injury caused by ROS. Fruits and vegetables are the best sources of natural antioxidants.<sup>15</sup> The carotenoid family comprises naturally pigmented antioxidants present in fruits and vegetables. Carotenoids are potent chemical quenchers of singlet oxygen ( $^1O_2$ ) and effective scavengers of other ROS.<sup>16</sup> Lycopene (lyco) is one of the most potent pigmented antioxidants among the dietary carotenoids: it effectively quenches singlet oxygen and free radicals to a greater extent than  $\beta$ -carotene, thereby shielding cells against free radical induced plasma membrane destruction and cell death.<sup>17</sup> Lyco and  $\beta$ -carotene are true hydrocarbons incorporated entirely within the inner surface of the cell membrane lipid bilayer; this integration is essential for preserving essential membrane characteristics, such as thickness, mechanical strength, stability, fluidity, and permeability, and maintaining proper function of the cell membrane.<sup>18</sup> Owing

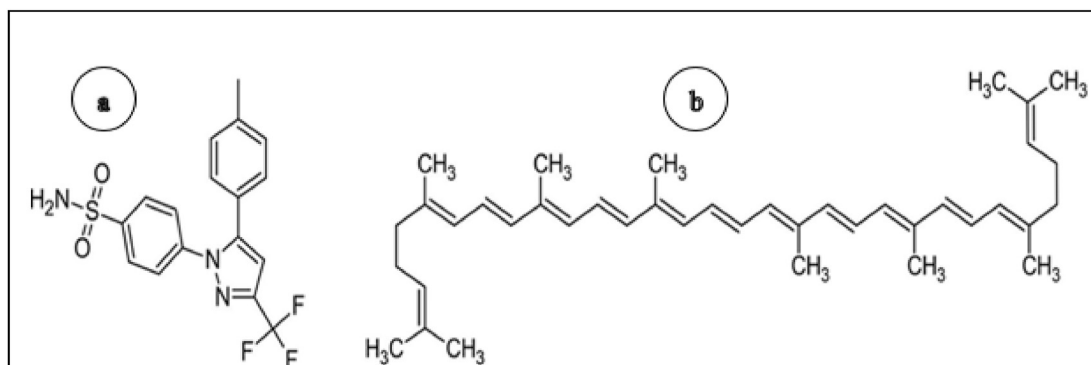


**Figure 1:** Structures of (a) celecoxib and (b) lycopene.

to its antioxidant potential, lyco minimizes cellular oxidative damage caused by disease or drugs.<sup>20</sup> Lyco is a phytonutrient naturally occurring in vegetables and fruits such as tomatoes, watermelons, pink guavas, grapefruits, apricots, and papayas.<sup>21</sup> This powerful antioxidant scavenges singlet oxygen and free radicals, and this activity underlies its health-promoting effects.<sup>22</sup>

Cb is an effective drug for treating fever, pain, and inflammation by selectively inhibiting COX-2; however, prolonged use of this drug may lead to toxic effects such as pericarditis in the cardiovascular system; fibrosis in the glomeruli of the kidneys; and substantial increases in serum enzymes such as alanine aminotransferase, aspartate aminotransferase, alkaline phosphatase, and total serum bilirubin.<sup>23</sup> Recent studies have revealed that oral intake of Cb markedly reduces ATP concentrations in hepatic mitochondria and is accompanied by increases in ADP concentrations. These variations may result in steatosis and eventually hepatocellular mitochondrial damage.<sup>24</sup>

Lyco has roles in maintaining cardiovascular health and preventing the occurrence of thrombotic conditions such as atherosclerosis.<sup>25</sup> Recent data have also revealed a neuroprotective role of lyco against bisphenol A exposed hippocampi in rats, because of its antioxidant properties.<sup>27</sup> Regular and long-term intake of lyco are associated with reduced risk of prostate cancer and other cancers, such as breast, colorectal and lung cancers.<sup>28</sup> Lyco has been shown to have cytoprotective effects against ischemic/reperfusion injury in a limb skeletal muscle model.<sup>29</sup> According to recent *in vitro* studies, lyco additionally has cartilage-protecting effects, given its anti-apoptotic, anti-inflammatory, and antioxidant properties.<sup>30</sup>

The liver, the largest gland in the body, is a vital organ performing more than 500 important functions. Critically, it filters the blood, and eliminates drugs and toxins from the circulation. The liver has a major role in metabolizing most drugs entering the circulation. Thus, this organ is continually exposed to risk while performing many functions critical for maintaining the health of the living human body. Any impairments in liver function may lead to increased accumulation of toxins, which endanger life. To maintain a healthy liver, adequate intake of supplements or antioxidants, whether natural or synthetic, is essential.<sup>31</sup>

Because of these important functions, we chose liver and hepatocyte samples as the main tissue specimens in this

study. Cb is a frequently prescribed potent anti-inflammatory medication. However, with prolonged use at high dosage, it can cause adverse effects on the liver, kidneys, and heart. Lyco, a member of the carotenoid family, has strong anti-inflammatory and antioxidant properties. This study was performed because no histological study had been conducted to elucidate whether concomitant use of lyco with Cb might minimize and reverse the toxic effects of Cb in the liver. Our study might also provide a basis for further investigation of the hepatotoxic effects of Cb on a molecular basis, and the reversal of these adverse effects through parallel supplementation with lyco. We further performed docking studies of lyco and Cb at COX-2 binding sites.

#### Materials and Methods

This experimental research was conducted (for 30 days) at the animal facility and research laboratory of the Department of Anatomy, Basic Medical Sciences Institute (BMSI), Jinnah Postgraduate Medical Centre (JPMC), Karachi. All procedures were in accordance with the Declaration of Helsinki,<sup>32</sup> and the study was approved by the institution's ethical committee under letter No. F.1-2/BMSI-E.COMT/JPMC. A total of 30 healthy, young adult male albino rats, 90–120 days of age, weighing 190–210 g, were selected and handled according to the guidelines of the US National Research Council's Guide for the Care and Use of Laboratory Animals. The rats were acclimated to the environment 1 week before the start of the study, and their health status and dietary intake were observed.<sup>33</sup> Cb was obtained in the form of Celbex capsules manufactured by Getz Pharma, and synthetic lyco was used in the form of soft gel capsules manufactured by General Nutrition Corporation (GNC). The calculated amounts of Cb and lyco to achieve experimental doses of 50 mg/kg body weight were administered orally through a feeding tube to the experimental animals.<sup>34</sup>

#### Administered dose of Cb in experimental animals

The calculated dose of Cb was 5 mg/100 g body weight. Oral doses were prepared as powder obtained from 100 mg Cb capsules dissolved in 10 ml normal saline. A 0.5 ml volume of the solution was administered per 100 g body weight.

The dose of lyco was 50 mg/kg body weight.

The dose calculation per 100 g body weight was as follows:

For 1 kg body weight, the dose of Cb was 50 mg.

$$1000 \text{ g} = 50 \text{ mg}$$

$$1 \text{ g} = 50/1000$$

$$100 \text{ g} = 50/1000 \times 100$$

$$100 \text{ g} = 5 \text{ mg}$$

$$50 \text{ g} = 2.5 \text{ mg}$$

$$25 \text{ g} = 1.25 \text{ mg}$$

The calculated dose of Cb was 5 mg/100 g body weight.

Oral doses were prepared as 100 mg Cb capsule (Getz Pharma) dissolved in 10 ml normal saline.

Because 10 ml normal saline contained 100 mg Cb.

$$10 \text{ ml} = 100 \text{ mg}$$

$$1 \text{ ml} = 100/10$$

$$1 \text{ ml} = 10 \text{ mg}$$

$$0.5 \text{ ml} = 5 \text{ mg}$$

An 0.5 ml solution volume was administered per 100 g body weight.

#### *Administered dose of lyco in experimental animals*

The calculated dose of lyco was 5 mg per/ 100 g of body weight. Oral doses were prepared as a gel by dissolving a 30 mg lyco capsule in corn oil, and the solution was then loaded into an insulin syringe with a total capacity of 60 units. Therefore, 10 units were administered per 100 g body weight.

Lyco doses were administered at 50 mg/kg body weight.

The dose calculation per 100 g body weight was as follows:

For 1 kg body weight, the dose of lyco was 50 mg.

$$1000 \text{ g} = 50 \text{ mg}$$

$$1 \text{ g} = 50/1000$$

$$100 \text{ g} = 50/1000 \times 100$$

$$100 \text{ g} = 5 \text{ mg}$$

$$50 \text{ g} = 2.5 \text{ mg}$$

$$25 \text{ g} = 1.25 \text{ mg}$$

The calculated dose of lyco was 5 mg/100 g body weight.

Oral doses were prepared as 30 mg lyco capsule (General Nutrition Corporation) dissolved in corn oil up to 60 units of insulin syringe.

Therefore,

$$60 \text{ units} = 30 \text{ mg}$$

$$1 \text{ unit} = 30/60$$

$$1 \text{ unit} = 0.5 \text{ mg}$$

$$2 \text{ units} = 1 \text{ mg}$$

$$4 \text{ units} = 2 \text{ mg}$$

$$6 \text{ units} = 3 \text{ mg}$$

$$8 \text{ units} = 4 \text{ mg}$$

$$10 \text{ units} = 6 \text{ mg}$$

Ten units per 100 g body weight was administered.

The test animals were categorized into the following groups:

**Group A:** control group receiving standard laboratory diet and water ad libitum.

**Group B:** administered Cb 50 mg/kg orally once daily.

**Group C:** administered Cb 50 mg/kg orally and lyco 50 mg/kg orally once daily.

All animals were weighed and housed in cages in a well-maintained room with a 12-h light/dark cycle in a laboratory environment. The animals were fed a standard laboratory diet and water ad libitum.<sup>35</sup> At the end of the treatment, all animals were again weighed and euthanized under ether anesthesia in a glass container. A midline longitudinal incision was made, and the abdominal viscera were carefully exposed. Gross features of the liver were noted, and the liver was removed from the body of each animal and weighed. The relative weight of the liver was calculated with the following formula.<sup>36</sup>

$$\text{The relative weight of liver} = \frac{\text{mean absolute weight of liver}}{\text{final weight of the animal}} \times 100$$

After weighing, the liver was washed with normal saline and cut into halves along the plane dividing it into left and right lobes. Both halves were preserved in buffered neutral formalin for 24 h. After fixation, tissues from the left half of the liver were processed and subjected to frozen sectioning with a cryostat-microtome. Frozen sections were obtained by rapid cooling of the tissue with a cryostat. The cryostat-microtome was used to rapidly freeze and subsequently slice the tissue for microscopic analysis. This prompt freezing of the tissue specimen converted the water into ice within the tissue, which served as an embedding medium for tissue slicing. Frozen sectioning of hepatic tissue was used primarily for lipid staining. Subsequently, 10  $\mu\text{m}$  thick sections were cut and placed on gelatinized glass slides, then stained with oil red O and hematoxylin\*.<sup>37</sup> The findings were rated as mild, moderate or severe on the basis of zonal distribution, according to the distribution area of glycogen in the hepatocytes in liver lobules. Zone I (Z-I) was the lobule region at the periphery, close to the portal triad; zone II (Z-II) was the region between zones I and II; and zone III (Z-III) was the area around the central vein. This procedure was performed to identify the fat content of hepatocytes according to the area affected. The amount of

fat varied inversely with the amount of glycogen. Grading<sup>38</sup> was determined as follows:

1. Mild: fat deposition in zone I (+)
2. Moderate: fat deposition in zones I and II (+ +)
3. Severe: fat deposition in zones I, II, and III (+ + +)

After fixation, tissue from the right half of the liver was processed by incubation in 70% alcohol overnight and dehydration with an ascending graded alcohol series. The liver tissue was cleared with xylene, then embedded in paraffin at 59 °C with a tissue embedding system. Subsequently, 4–5 µm thick sections of hepatic tissues were stained with hematoxylin and eosin to measure the diameters of hepatocytes and their nuclei, and with periodic acid Schiff (PAS) and hematoxylin\* to observe the glycogen content of hepatocytes.<sup>37</sup> The findings were scored as mild, moderate, or severe on the basis of the area of distribution of glycogen in hepatocytes in all three liver lobule zones. The deposition of glycogen was inversely proportional to the distribution of fat in hepatocytes. The findings were scored<sup>38</sup> as follows:

4. Mild: glycogen depletion in zone I (+)
5. Moderate: glycogen depletion in zones I and II (+ +)
6. Severe: glycogen depletion in zones I, II, and III (+ + +)

The tissue sections were examined under the 40× objective of a light microscope, and the results were analyzed.

#### *Hematoxylin and eosin staining procedure*

The tissue sections were deparaffinized with xylene, then hydrated with a descending alcohol series. The slides were immersed in Harris hematoxylin solution for several minutes, then washed well in water until the water appeared clear. The sections were stained with eosin and washed with water until the water became clear. The tissue sections were then dehydrated with a graded alcohol series, cleared with xylene, and mounted in di-n-butyl phthalate in xylene.<sup>37</sup>

#### *PAS and hematoxylin staining procedure*

The tissue sections were deparaffinized in xylene and rehydrated with a descending graded alcohol series, then treated with periodic acid solution. Thereafter, specimen-containing glass slides were rinsed well in distilled water and covered with Schiff reagent, and subsequently rinsed with water for several minutes. The tissue sections were then covered with Harris hematoxylin to stain the nuclei. The tissue sections were dehydrated in an ascending graded alcohol series, cleared with xylene, and mounted in di-n-butyl phthalate. The slides were observed under a microscope. The periodic acid reactive material, i.e., the glycogen content of hepatocytes, appeared magenta, and their nuclei appeared blue.<sup>37</sup>

#### *Oil red O and hematoxylin staining procedure*

The frozen tissue sections were stained with freshly prepared oil red O working solution for 15–20 minutes, then rinsed with water until all excess water was removed. The frozen sections were counter-stained with Gill's hematoxylin for approximately 1 min, then rinsed with water several times. The sections were mounted on a coverslip with

aqueous mounting medium. The slides were subsequently observed under a microscope. The lipid droplets appeared red, and the nuclei appeared blue.<sup>37</sup>

#### *Micrometric calculation of hepatocyte diameter and hepatocyte nuclear diameter*

Micrometry was performed with a stage micrometer and ocular micrometer scale. The stage micrometer was used for calibration of the ocular micrometer scale. The stage micrometer used for this purpose was 1 mm long and was divided into 100 divisions of 10 µm each. The ocular micrometer scale was placed in the right eyepiece of a light microscope.

#### *Calibration of the ocular micrometer with the stage micrometer under a 100× objective*

The ocular micrometer scale coincided with the stage micrometer scale under an 8× ocular and 100× objective; 50 small divisions of the ocular micrometer scale coincided with five divisions of the micrometer scale, which were equal to 50 µm. Therefore, one small division of the ocular micrometer was equal to 1 µm under a 100× objective and 8× ocular.

#### *Statistical analysis*

The statistical significance of differences in various quantitative data between treated and control rats were calculated with Student's t-test. SPSS-20 was used for statistical analysis. Differences were considered statistically significant if the P-value was ≤0.05.

#### *Docking studies*

##### *Preparation of ligands and protein*

For docking, 3D structures of lyco and Cb were obtained from the PubChem database<sup>39</sup> in a suitable format (PDB) and served as ligands. The target protein, PDB ID: 3LN1 (structure of Cb bound at the COX-2 active site), with a resolution of 2.40 Å, was downloaded from the RCSB Protein Data Bank and prepared for docking by removal of water molecules and co-crystallized ligands in PyMOL software.

##### *Molecular docking*

Molecular docking studies were performed in the AutoDock Vina 4.2.6 software package. To specify the binding sites, we generated a centroid grid box encompassing the binding site for docking calculations. The binding sites for 3LN1 were GLN:178, ARG:499, LEU:345, SER:339, and ARG:106. The docked protein-ligand complexes were ranked according to their predicted binding energies.<sup>40</sup>

##### *Screening criteria*

The goal of the present research was to provide an in silico demonstration that concomitant intake of lyco with Cb prevents hepatotoxic effects. The molecular docking results were visualized and analyzed with the PyMOL molecular visualization tool.

## Results and discussion

This study was designed primarily to observe the potential harmful effects of Cb alone and the effects of lyco in ameliorating Cb induced damage in the liver in an experimental rat model. This aim was achieved by examination of gross changes, such as increases or decreases in relative liver weight, as well as the histomorphology of the liver, as observed under a light microscope. The histological examination was followed by appropriate staining of hepatic tissue to observe fatty degeneration and glycogen depletion in hepatocytes after administration of Cb either alone or together with lyco.

**Group A:** The mean relative weight of the liver was  $3.30 \pm 0.10$  g/100 g (Table 1). The mean hepatocyte diameter in group A was  $16.2 \pm 0.83$   $\mu$ m (Table 4), whereas the mean hepatocyte nuclear diameter was  $7.2 \pm 0.27$   $\mu$ m (Table 5). Frozen sections of liver stained with oil red O and hematoxylin showed occasional deposition of fat within hepatocytes, primarily in periportal areas [Figure 2(a), Table 2]. Liver sections stained with PAS and hematoxylin showed a normal and uniform distribution of glycogen throughout the hepatic lobules [Figure 2(b), Table 3].

**Group B:** The mean relative weight of the liver was  $4.99 \pm 0.23$  g/100 g. The relative liver weight was highly significantly greater ( $P < 0.001$ ) in group B than control group A (Table 1). The mean hepatocyte diameter in group B was  $23.6 \pm 0.96$   $\mu$ m and was highly significantly larger ( $P < 0.001$ ) than that in control group A (Table 4). The mean hepatocyte nuclear diameter in group B was  $4.7 \pm 0.27$   $\mu$ m and was highly significantly smaller ( $P < 0.001$ ) than that in control group A (Table 5). Sections of liver tissue stained with oil red O and hematoxylin showed severe (+ + +) fatty infiltration within the hepatocytes of group B, in comparison to control group A. This infiltration involved all three zones, extending from periphery/periportal areas (Z-I) to the center/central vein (Z-III) of the hepatic lobules [Figure 2(c), Table 2]. Similarly, sections of liver tissue stained with PAS and hematoxylin in group B, as compared with control group A, showed marked (+ + +) glycogen depletion in the hepatocytes, extending from periportal areas (Z-I) to the central vein (Z-III) of the hepatic lobules [Figure 2(d), Table 3].

**Group C:** The mean absolute liver weight in group C, treated with Cb with lyco, was  $3.32 \pm 0.07$  g/100g. The relative liver weight in group C was non-significantly higher ( $P > 0.05$ ) than that in control group A. The relative liver weight of group C was highly significantly lower ( $P < 0.001$ ) than that in group B (Table 1). The mean hepatocyte diameter in group C was  $17.2 \pm 1.44$   $\mu$ m. The mean diameter of hepatocytes of group C was significantly larger ( $P < 0.05$ ) than that in control group A. The mean hepatocyte diameter was moderately significantly smaller ( $P < 0.005$ ) in group C than group B (Table 4). The mean nuclear diameter of hepatocytes in group C was  $6.4 \pm 0.22$   $\mu$ m. The nuclear diameter in group C was significantly smaller ( $P < 0.05$ ) than that in control group A, but moderately significantly larger ( $P < 0.005$ ) than that in group B (Table 5). Oil red O stained frozen liver sections showed mild (+) fatty infiltration in the periportal areas of hepatocytes [Figure 2(e), Table 2]. Reciprocally, PAS and hematoxylin stained liver sections in group C showed minimal (+) glycogen reduction in the periportal areas of hepatic lobules [Figure 2(f), Table 3].

In vitro studies are rapid, economical, simple, and species specific, yet physiologically limited, whereas in vivo studies are more specific and reliable for observing biological effects in animals. We believe that Cb and lyco may have comparable effects in terms of human physiology. However, this aspect is a limitation of our study and should be further evaluated in human models at the molecular level. It can be useful to advance drug development research in such a manner that the animal studies should be performed beforehand to provide medical researchers with a better approximation of a drug or chemical's health promoting effects as well as the toxic effects likely to be observed in humans.

The liver is a principal site responsible for uptake, concentration, metabolism, and elimination of a large variety of drugs. This highly metabolically active organ contains many important enzymes. Because most of the drugs entering the circulation pass through the liver, any new drug or chemical—such as analgesic, anti-inflammatory, anti-hypertensive, antibiotic or antioxidant agents—should be evaluated in terms of liver pharmacodynamics by using an in vivo system before use of in vitro models.

In this experiment, markedly greater absolute and relative liver weights were observed in Cb treated group B animals than control animals. This finding might have been due to steatosis and steatohepatitis occurring as a result of increased fatty infiltration and inflammatory mediators.<sup>41</sup>

Lyco decreased and restored the absolute and relative liver weights in group C animals. This finding might have been because its anti-hyperlipidemic and anti-inflammatory hepatoprotective effects ameliorated drug induced steatosis and steatohepatitis, as described by Bahcecioglu et al., in 2010,<sup>42</sup> in a study indicating that lyco prevents induction of steatohepatitis by a high-fat diet.

In this study, oil red O and hematoxylin-stained liver sections of Cb treated animals showed marked fatty infiltration and steatosis, whereas PAS and hematoxylin-stained liver sections showed marked depletion of glycogen in all three hepatic lobule zones. Fat deposition in the hepatocytes is inversely proportional to glycogen depletion.<sup>38</sup> Group B animals showed fatty infiltration of the liver caused by the

**Table 1: Mean relative weight of liver (g/100 g) in groups of albino rats.**

Groups	Treatment	Mean relative weight of liver
A (n = 10)	ND	$3.30 \pm 0.10$
B (n = 10)	Cb	$4.99 \pm 0.23$
C (n = 10)	Cb + lyco	$3.32 \pm 0.07$
<b>Statistical comparison</b>		<b>P-value</b>
B vs. A		$P < 0.001****$
C vs. A		$P > 0.05^*$
C vs. B		$P < 0.001****$

**Key:** ND, normal diet; non-significant\*; significant\*\*; moderately significant\*\*\*; highly significant\*\*\*\*.

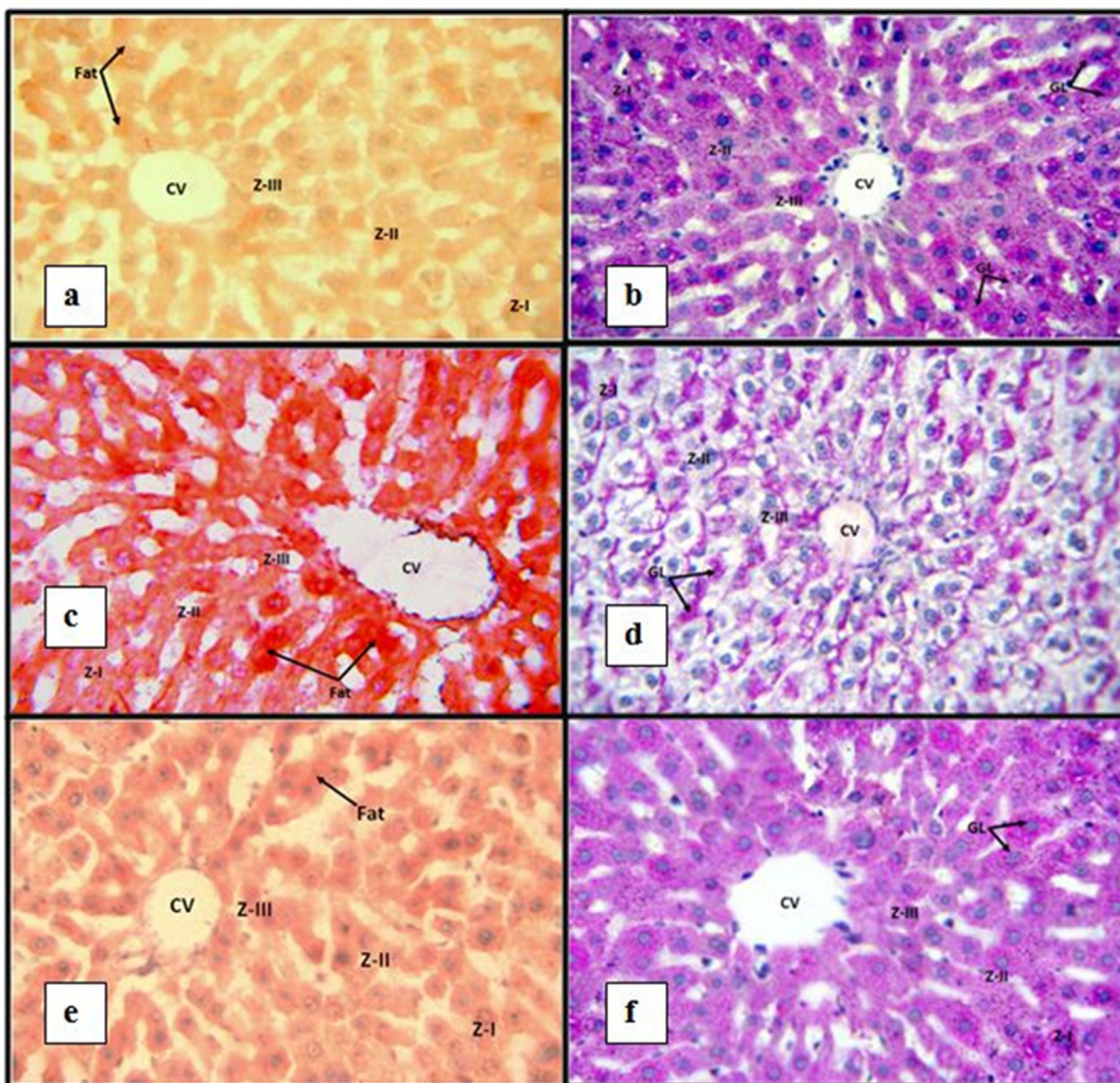


**Figure 2:** Light micrographs of rat liver sections in the control, Cb treated, and Cb + lycopene treated groups stained with oil red O and hematoxylin (a, c, and e), scale bar = 10  $\mu\text{m}$ , and PAS and hematoxylin (b, d, and f), scale bar = 4  $\mu\text{m}$  (400 $\times$ ). (a) Liver section from a control rat, showing the zonal distribution of hepatic lobules (Z-I, Z-II, and Z-III) around the central vein (CV) with occasional fat deposition, and (b) regular glycogen (GL) content in hepatocytes. (c) Liver section from a Cb treated rat, showing marked fat deposition and (d) marked depletion of GL in all three hepatic lobule zones. (e) Liver section from a Cb + lycopene treated rat, showing mild fat accumulation around the CV and (f) minimal GL depletion in the periportal areas of the hepatic lobule.

Cb, because enhanced lipogenesis and lipid peroxidation led to increased fat deposition in hepatocytes.<sup>12</sup> Similar findings were reported by Ebaid et al., in 2006,<sup>43</sup> in a study indicating that fat deposition inversely replaced the glycogen in hepatocytes and resulted in glycogen depletion in COX-2 inhibitor treated mice.

Group C animals showed markedly reduced fat deposition, because of the protective effects of lycopene, as described by Bahcecioğlu et al. in 2010.<sup>42</sup> In that study, the hypocholesteremic effect of lycopene was found to be due to inhibition of the HMG Co-A reductase enzyme and a decrease in fat deposition in cells. The same group has reported significant reversal of glycogen depletion in

hepatocytes, as reported by Mansour et al. in 2011,<sup>17</sup> in a study demonstrating the protective effects of lycopene against oxidative stress caused by sodium fluoride and gamma radiation.

We observed markedly greater hepatocyte diameters in Cb treated group B animals than control animals, possibly because of fatty infiltration and increased levels of inflammatory mediators.<sup>44</sup> Increased diameters of swollen hepatocytes are indicative of inflammation leading to hepatocyte damage. This observation was complemented by a highly significant decrease in hepatocyte nuclear diameter, indicating shrinkage or pyknosis, possibly because Cb reduces cell proliferation, angiogenesis, and the

**Table 2: Fat content of hepatocytes in groups of albino rats.**

Groups	Treatment	Fat deposition in different liver zones		
		Mild	Moderate	Severe
A (n = 10)	ND	–	–	–
B (n = 10)	Cb	–	–	+++
C (n = 10)	Cb + lyco	+	–	–

**Key:** ND, normal diet; mild, Z-I; moderate, Z-I + II; marked, Z-I + II + III.

**Table 3: Glycogen content of hepatocytes in groups of albino rats.**

Groups	Treatment	Glycogen depletion in various liver zones		
		Mild	Moderate	Severe
A (n = 10)	ND	–	–	–
B (n = 10)	Cb	–	–	+++
C (n = 10)	Cb + lyco	+	–	–

**Key:** ND, normal diet; mild, Z-I; moderate, Z-I + II; marked, Z-I + II + III.

production of antioxidative enzymes causing oxidative damage to cells, and increases tumor necrosis factor- $\alpha$ , thereby resulting in apoptosis or cell death.<sup>41</sup>

In the lyco protected animals in group C, the hepatocyte and nuclear diameters were restored to values near those in controls, because of this compound's antioxidant and anti-inflammatory effects, as verified by El-Sayed et al. in 2015.<sup>45</sup> In that study, lyco was found to exert antioxidative and anti-inflammatory effects by restoring the antioxidant enzymes. Lyco decreased lipid peroxidation and protected against free radical induced cell damage, thus restoring the hepatocyte and nuclear diameters to near-normal sizes.

The increased diameters of swollen hepatocytes of animals receiving Cb indicated inflammation leading to hepatocyte damage, whereas the considerable decreases in nuclear diameter indicated shrinkage or pyknosis followed by apoptosis or cell death. The restoration of the diameters of ballooned hepatocytes and the restoration of the decreased diameters of shrunken nuclei to normal values after simultaneous administration of lyco with Cb indicated the protective action of lyco against Cb induced hepatocyte damage.

Hence, we conclude that the concomitant use of lyco may ameliorate Cb induced fatty degeneration and glycogen depletion in hepatocytes. Cb was verified to cause oxidative injury in hepatic tissue, via increased lipid peroxidation and inhibition of oxidative phosphorylation, thus resulting in ROS formation. Oxidative stress plays a key role in the

**Table 5: Mean hepatocyte nuclear diameter ( $\mu\text{m}$ ) in groups of albino rats.**

Groups	Treatment	Mean hepatocyte nuclear diameter
A (n = 10)	ND	7.2 $\pm$ 0.27
B (n = 10)	Cb	4.7 $\pm$ 0.27
C (n = 10)	Cb + lyco	6.4 $\pm$ 0.22
<b>Statistical comparison</b>		<b>P-value</b>
B vs. A		P < 0.001****
C vs. A		P > 0.05**
C vs. B		P < 0.005***

**Key:** ND, normal diet; non-significant\*; significant\*\*; moderately significant\*\*\*; highly significant\*\*\*\*.

pathogenesis of fatty liver/steatosis and hypercholesterolemia, which may progress to steatohepatitis, fibrosis, cirrhosis, and finally end-stage liver diseases such as hepatocellular carcinoma. The mechanisms through which ROS mediate the development of fatty liver may be indiscriminate oxidative biomolecular injury and dysregulated redox signaling, but these possibilities remain to be further evaluated. Lyco, a phytochemical and a potent natural antioxidant, is a strong scavenger of singlet oxygen and other ROS, because its chemical structure has numerous double bonds, as illustrated in Figure 1(b), which have a key role in ROS scavenging.<sup>19</sup> Moreover, evidence suggests that lyco markedly reduces LDL cholesterol, thus decreasing systolic blood pressure.<sup>26</sup> Our study demonstrated that lyco ameliorates hepatocyte deterioration in a rat model of Cb treatment, and fat accumulation along with glycogen loss in hepatocytes. Because of its antioxidant potential, lyco minimizes the oxidative damage to cells caused by disease or drugs.<sup>20</sup> Given its health promoting effects demonstrated herein, the natural product lyco may be used as a synthetic drug candidate or dietary supplement for scavenging singlet oxygen and other reactive species.

#### Docking studies

We conducted molecular docking studies to evaluate the potential binding interactions of Cb and lyco with the target protein. The structure of COX-2 bound to Cb was downloaded from the RCSB Protein Data Bank, under PDB code 3LN1.<sup>46</sup> AutoDock Vina 4.2.6 was used for docking. Both ligands were docked into the binding site of 3LN1. The binding affinities of the lyco and Cb ligands were calculated to be  $-7.3$  kcal/mol and  $-7.9$  kcal/mol, respectively, as shown in Table 6. These values indicated the predicted strength of the binding interaction between the ligands and the protein. The highly negative binding

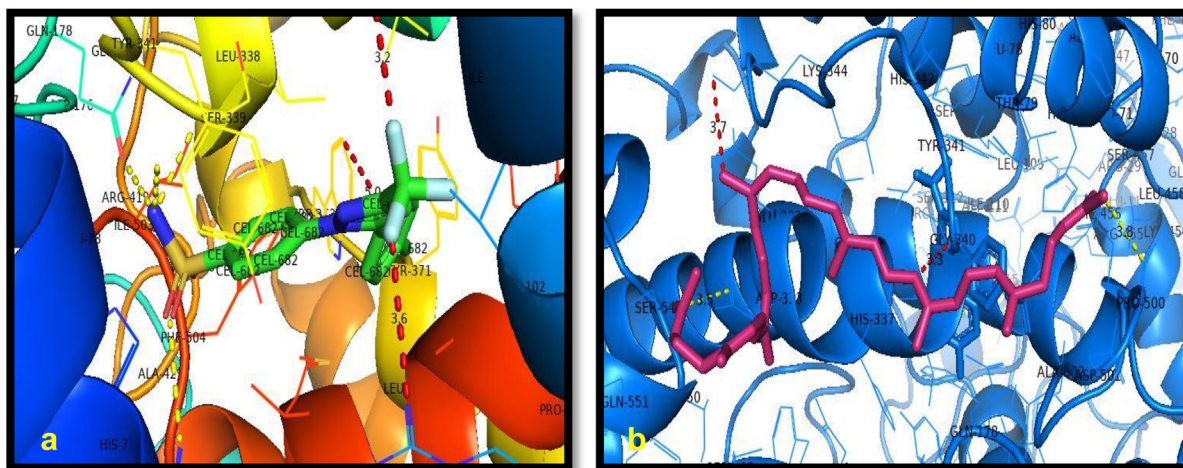
**Table 4: Mean hepatocyte diameter ( $\mu\text{m}$ ) in groups of albino rats.**

Groups	Treatment	Mean hepatocyte diameter	Statistical comparison	P-value
A (n = 10)	ND	16.2 $\pm$ 0.83	B vs. A	P < 0.001****
B (n = 10)	Cb	23.6 $\pm$ 0.96	C vs. A	P < 0.05**
C (n = 10)	Cb + lyco	17.2 $\pm$ 1.44	C vs. B	P < 0.005***



**Table 6: Hydrogen and hydrophobic interactions with binding affinities at the active site of target 3LN1.**

Ligands	Binding affinity	No. of hydrogen bonding interactions	Amino acid involved in hydrogen bonding, and bond length	No. of hydrophobic bonds	Amino acid involved in hydrophobic bonding
Cb	-7.9	02	Gln178 (3.1) Arg499 (3.3)	03	Leu345 (3.6) Ser339 (4.0) Arg106 (3.6)
Lycy	-7.3	02	Asp333 (3.5) Pro500 (3.8)	02	Lys344 (3.5) Gly340 (3.3)

**Figure 3:** Hydrogen bonding and hydrophobic bonding interactions of (a) celecoxib and (b) lycopene at the active site of the 3LN1 target.

affinities of both Cb and lycy indicated strong interactions with COX-2. The calculated binding affinities indicated significant binding strength. Strong binding affinity implied effective inhibition of the COX-2 activity associated with inflammatory processes. In [Figure 3\(a\)](#), the 3D diagram shows the ligand Cb in stick form in green, whereas in [\(b\)](#), the ligand lycy is in pink with numbered amino acid residues. Both diagrams show hydrogen bonding as dotted yellow lines and hydrophobic bonding as dotted red lines. This 3D figure of ligand and target interactions was created in PyMOL.<sup>47</sup> Lycy had a binding affinity of  $-7.3$  kcal/mol, thus suggesting that it forms hydrogen bonds with residues Asp333, with bond length  $3.5$  Å, and Pro500, with bond length  $3.8$  Å. Lycy also engages in hydrophobic interactions with residues Lys344, with bond length  $3.7$  Å, and Gly340, with bond length  $3.3$  Å, as shown in [Table 6](#). These interactions indicate the potential stability and specificity of the lycy-protein complex.

Cb exhibited a slightly higher binding affinity of  $-7.9$  kcal/mol. Docking studies indicated that Cb forms hydrogen bonds with residues Gln178, with bond length  $3.1$  Å, and Arg499, with bond length  $3.3$  Å. Additionally, hydrophobic interactions were observed with residues Leu345, with bond length  $3.6$  Å; Ser339, with bond length  $4.0$  Å; and Arg106, with bond length  $3.6$  Å. Comparison of the binding affinities of lycy and Cb indicated that both ligands exhibited strong binding interactions with the target protein 3LN1. This study suggested that both Cb and lycy may serve as potential COX-2 inhibitors with implications

for anti-inflammatory therapy. The detailed analysis of binding affinities and specific interactions (hydrogen bonding and hydrophobic bonding) provide valuable information and broader understanding of the molecular mechanisms underlying inflammation, and offer insights into the design of targeted therapies for inflammatory diseases.

## Conclusion

Despite the effectiveness of Cb as an analgesic and anti-inflammatory drug, prolonged high-dose use can lead to hepatic tissue injury, probably because of oxidative stress and fatty degeneration. This study demonstrated that lycy significantly mitigates fat deposition and glycogen depletion in hepatocytes, and thus may protect against hepatocellular damage. Additionally, docking studies showed strong binding interactions of Cb and lycy with the target protein 3LN1, with binding affinities of  $-7.3$  kcal/mol and  $-7.9$  kcal/mol, respectively. Importantly, our findings suggested that the concomitant intake of lycy, a natural product, along with Cb, a synthetic drug, may decrease Cb induced fat deposition and glycogen reduction in liver cells.

## Source of funding

This research did not receive any specific grant from funding agencies in the public, commercial, or not-for-profit sectors.

## Conflict of interest

The authors have no conflict of interest to declare.

## Ethical approval

According to the Institutional Review Board Statement, all procedures in the study were performed in accordance with the Declaration of Helsinki, and the study was approved by the Jinnah Postgraduate Medical Centre (JPMC) ethical committee under letter No. F.1-2/BMSI-E.COMT/JPMC.

## Authors contributions

MK conceived and designed the study, conducted research, provided research materials, and collected and organized data. SG analyzed and interpreted data, and supervised the study. MK and SG wrote the initial and final drafts of the article, and provided logistic support. IR and SG conducted docking studies. All authors have critically reviewed and approved the final draft and are responsible for the content and similarity index of the manuscript.

## References

- Nikolic M, Sustersic T, Filipovic N. In vitro models and on-chip systems: biomaterial interaction studies with tissues generated using lung epithelial and liver metabolic cell lines. *Front Bioeng Biotechnol* 2018 Sep 3; 6: 120.
- Hiemstra PS, Grootaers G, van der Does AM, Krul CAM, Kooter IM. Human lung epithelial cell cultures for analysis of inhaled toxicants: lessons learned and future directions. *Toxicol In Vitro* 2018; 47: 136–147.
- Cho S, Yoon JY. Organ-on-a-chip for assessing environmental toxicants. *Curr Opin Biotechnol* 2017; 45: 34–42.
- Visha MG. Selective COX-2 inhibitor. *Int J Pharma Sci* 2013; 3: 28–33.
- Suleyman H, Demircan B, Karagoz Y. Anti-inflammatory and side effects of cyclooxygenase inhibitors. *Pharmacol Rep* 2007; 59: 247–258.
- Niranjana R, Manik P, Srivastava AK, Palit G, Natu SM. Comparative adverse effects of COX-1 and COX-2 inhibitors in rat liver: an experimental study. *J Anat Soc India* 2010; 59: 182–186.
- Gong L, Thorn CF, Bertagnoli MM, Grosser T, Altman RB, Klein TE. Celecoxib pathways: pharmacokinetics and pharmacodynamics. *Pharmacogenetics Genom* 2012; 22: 310–318.
- Davies NM, McLachlan AJ, Day RO, Williams KM. Clinical pharmacokinetics and pharmacodynamics of celecoxib: a selective cyclooxygenase-2 inhibitor. *Clin Pharmacokinet* 2000; 38: 225–242.
- Mukthinthalapati PK, Fontana RJ, Vuppalanchi R, Chalasani N, Ghahril M. Celecoxib-induced liver injury. *J Clin Gastroenterol* 2018; 52: 114–122.
- Sriuttha P, Sirichanchuen B, Permsuwan U. Hepatotoxicity of nonsteroidal anti-inflammatory drugs: a systematic review of randomized controlled trials. *Int J Hepatol* 2018; 1–13.
- Schmeltzer PA. Drug-induced liver injury due to non-steroidal anti-inflammatory drugs. *Curr Hepatol Rep* 2019; 18: 294–299.
- Mahmood KS, Ahmed JH, Jawad AM. Non steroidal anti-inflammatory drugs (NSAIDs), free radicals and reactive oxygen species (ROS): a review of literature. *MJBU* 2009; 27: 46–53.
- Chen Z, Tian R, Shea Z, Cai J, Li H. Role of oxidative stress in the pathogenesis of nonalcoholic fatty liver disease. *Free Radic Biol Med* 2020; 152: 116–141.
- Nair P, Kanwar SS, Sanyal SN. Effects of non steroidal anti-inflammatory drugs on the antioxidant defense system and the membrane functions in the rat intestine. *Nutr Hosp* 2006; 21: 638–649.
- Dillingham BL, Rao AV. Biologically active lycopene in human health. *Int JNM* 2009; 4: 23–27.
- Imran M, Ghorat F, Haq I, Rehman H, Aslam F, Heydari M, et al. Lycopene as a natural antioxidant used to prevent human health disorders. *Antioxidants* 2020; 706: 1–27.
- Mansour HH, El Azeem MG, Ismael NE. Role of lycopene against hepatorenal oxidative stress induced by sodium fluoride and gamma rays. *J Radiat Res Appl Sci* 2011; 4: 435–460.
- Rocha DFA, Machado-Junior PA, Souza ABF, Castro TF, Costa GP, Talvani A, et al. Lycopene ameliorates liver inflammation and redox status in mice exposed to long-term cigarette smoke. *BioMed Res Int* 2021; 1–11.
- Elsayed A, Elkomy A, Elkammar R, Youssef G, Abdelhiee EY, Abdo W, et al. Synergistic protective effects of lycopene and N-acetylcysteine against cisplatin-induced hepatorenal toxicity in rats. *Sci Rep* 2021; 11: 1–10.
- Agarwal S, Rao AV. Tomato lycopene and its role in human health and chronic diseases. *Can Med Assoc J* 2000; 163: 739–744.
- Wadie W, Mohamed AH, Masoud MA, Rizk HA, Sayed HM. Protective impact of lycopene on ethinylestradiol-induced cholestasis in rats. *Naunyn-Schmiedeb Arch Pharmacol* 2020; 394: 447–455.
- Adikwu E, Bokolo B. Lycopene restores liver function and morphology of ifosfamide-intoxicated rats. *Arch Med Health Sci* 2019; 7: 13–17.
- Aziz ND, Ouda MH, Ubaid MM. Comparing the toxic effects of nonsteroidal anti-inflammatory drugs (celecoxib and ibuprofen) on heart, liver, and kidney in rats. *Asian J Pharm Clin Res* 2018; 11: 482–485.
- Sulimani ES, Yousef JM, Mohamed AM. Molecular target mechanisms of celecoxib induced liver damage in rats and the potential prophylactic roles of melatonin and/or quercetin. *J Pharm Pharmacogn Res* 2021; 9: 397–408.
- Saini RK, Rengasamy KRR, Mahomoodally FM, Keum YS. Protective effects of lycopene in cancer, cardiovascular, and neurodegenerative diseases: an update on epidemiological and mechanistic perspectives. *Pharmacol Res* 2020; 155: 1–16.
- Hsieh MJ, Huang CY, Kiefer R, Lee SD, Maurya N, Velmurugan BK. Cardiovascular disease and possible ways in which lycopene acts as an efficient cardio-protectant against different cardiovascular risk factors. *Molecules* 2022; 27: 1–16.
- El Morsy EM, Ahmed MAE. Protective effects of lycopene on hippocampal neurotoxicity and memory impairment induced by bisphenol A in rats. *Hum Exp Toxicol* 2020; 39: 1066–1078.
- Rowles JL, Ranard KM, Smith JW, An R, Erdman Jr JW. Increased dietary and circulating lycopene are associated with reduced prostate cancer risk: a systematic review and meta-analysis. *Prostate Cancer Prostatic Dis* 2017; 20: 361–377.
- Kirişçi M, Güneri B, Seyithanoğlu M, Kazancı U, Doğaner A, Güneş H. The protective effects of lycopene on ischemia/reperfusion injury in rat hind limb muscle model. *Turk J Trauma Emerg* 2020; 26: 351–360.
- Wu Z, Zhang X, Li Z, Wen Z, Lin Y. Activation of autophagy contributes to the protective effects of lycopene against oxidative stress-induced apoptosis in rat chondrocytes. *Phytother Res* 2021; 35: 4032–4045.
- Trefts E, Gannon M, Wasserman DH. The liver. *Curr Biol* 2017; 27: 1–10.

32. Carlson RV, Boyd KM, Webb DJ. The revision of the Declaration of Helsinki: Past, present and future. **Br J Clin Pharmacol** 2004; 57: 695–713.
33. Committee for the update of the Guide for the Care and Use of laboratory animals. *Guide for the care and use of laboratory animals*. 8th ed. Washington DC, USA: National Research Council of the National Academies, The National Academies Press; 2011. pp. 42–75, 115–121, 136–141.
34. Khan M, Gul S, Abdul Haq A, Rafiq K, Leghari Q, Memon FM. Protective effect of lycopene on celecoxib induced hepatotoxicity in albino rats: a histological study. **Pak J Pharm Sci** 2020; 33(Suppl.): 1215–1220.
35. Hemieda FAE, Hassan HA, Ibrahim EE, Mashaly MA. Protective impact of lycopene on flutamide-induced hepatotoxicity in male rats. **Egypt. J Exp Biol** 2017; 13: 1–7.
36. Eleazu CO, Iroaganachi M, Okafor PN, Ijeh II, Eleazu KC. Ameliorative potentials of ginger (*Z. officinale* Roscoe) on relative organ weights in streptozotocin induced diabetic rats. **Int J Biomed** 2013; 9: 82–90.
37. Bancroft JD, Gamble M. *Theory and practice of histological techniques*. 6th ed. London, UK: Churchill Livingstone Elsevier; 2008. pp. 68, 84–86, 98–99, 126–127, 171, 193–194.
38. Qamar A, Siddiqui A, Kumar H. Fresh garlic amelioration of high-fat-diet induced fatty liver in albino rats. **J Pak Med Assoc** 2015; 65: 1102–1107.
39. Kim S, Chen J, Cheng T, Gindulyte A, He J, He S, et al. PubChem 2019 update: improved access to chemical data. **Nucleic Acids Res** 2019; 47(D1): D1102–D1109.
40. Forli S, Huey R, Pique ME, Sanner MF, Goodsell DS, Olson AJ. Computational protein–ligand docking and virtual drug screening with the AutoDock suite. **Nat Protoc** 2016; 11(5): 905–919.
41. Somanath D, Sowmya PS. Comparative adverse effects of aceclofenac and celecoxib on liver of wistar albino rats. **IJBAMR** 2014; 3: 303–307.
42. Bahcecioglu IH, Kuzu N, Metin K, Ozercan IH, Ustundag B, Sahin K, et al. Lycopene prevents development of steatohepatitis in experimental nonalcoholic steatohepatitis model induced by high-fat diet. **Vet Med Int** 2010; 1–8.
43. Ebaid H, Dkhil MA, Danfour MA, Tohamy A, Gabry MS. Piroxicam-induced hepatic and renal histopathological changes in mice. **Libyan J Med** 2006; 2: 82–89.
44. Bykov IL, Palmen M, Rainsford KD, Lidros KO. Chronic effects of celecoxib, a cyclooxygenase-2 inhibitor, cause enhanced alcohol-induced liver steatosis in rats. **Inflammopharmacology** 2005; 0: 1–11.
45. El-Sayed EM, Fouda EE, Mansour AM, Elazab AH. Protective effect of lycopene against carbon tetrachloride-induced hepatic damage in rats. **Int J Pharma Sci** 2015; 5: 875–881.
46. Wang JL, Limburg D, Graneto MJ, Springer J, Hamper JR, Liao S, et al. The novel benzopyran class of selective cyclooxygenase-2 inhibitors. Part 2: the second clinical candidate having a shorter and favorable human half-life. **Bioorg Med Chem Lett** 2010 Dec 1; 20(23): 7159–7163.
47. Schrödinger L. *The PyMOL molecular graphics system, version 2.0*. Schrödinger, LLC; 2017.

**How to cite this article:** Khan M, Gul S, Rehman I, Leghari Q-a, Badar R, Zille-Huma. Protective effect of lycopene against celecoxib induced fat deposition and glycogen reduction in liver cells. *J Taibah Univ Med Sc* 2024;19(4):856–866.